

# On a New $(21_4)$ Polycyclic Configuration

Leah Wrenn Berman<sup>a</sup>      Gábor Gévay<sup>b</sup>      Tomaž Pisanski<sup>c,d</sup>

Submitted: Sept 22, 2023; Accepted: Oct 20, 2024; Published: Nov 29, 2024

© The authors. Released under the CC BY-ND license (International 4.0).

## Abstract

When searching for small 4-configurations of points and lines, polycyclic configurations, in which every symmetry class of points and lines contains the same number of elements, have proved to be quite useful. In this paper we construct and prove the existence of a previously unknown  $(21_4)$  configuration, which provides a counterexample to a conjecture of Branko Grünbaum. In addition, we study some of its most important properties; in particular, we make a comparison with the well-known Grünbaum–Rigby configuration. We show that there are exactly two  $(21_4)$  geometric polycyclic configurations and seventeen  $(21_4)$  combinatorial polycyclic configurations. We also discuss some possible generalizations.

**Mathematics Subject Classifications:** 51A45, 51A20, 05B30, 51E30, 05C62

## 1 Introduction

A breakthrough in the modern study of geometric configurations of points and lines came with the seminal paper [17] of Grünbaum and Rigby in which the first geometric point-line representation of a 4-configuration was constructed. This  $(21_4)$  configuration, which has 21 points and lines in which each point lies on 4 straight lines and each line passes through four points, was based on the work of Felix Klein [19] on his famous quartic curve, and is nowadays known as the Grünbaum–Rigby configuration; we denote it by  $\text{GR}(21_4)$ . Later, Branko Grünbaum discovered a large number of  $(n_4)$  configurations. Some of them were constructed in the spirit of  $\text{GR}(21_4)$  (later called *celestial* configurations), while others were constructed by various techniques from smaller ones. In 2003, Boben and Pisanski [6] initiated the theory of *polycyclic configurations*, having  $\text{GR}(21_4)$  and some other configurations from another paper of Grünbaum (co-authored by Harold Dorwart) [13] as the prime models of such configurations.

---

<sup>a</sup>Department of Mathematics & Statistics, University of Alaska Fairbanks, Fairbanks, U.S.A. (lwberman@alaska.edu).

<sup>b</sup>Bolyai Institute, University of Szeged, Szeged, Hungary (gevay@math.u-szeged.hu).

<sup>c</sup>FAMNIT, University of Primorska, Koper, Slovenia (tomaz.pisanski@upr.si).

<sup>d</sup>Institute of Mathematics, Physics and Mechanics, Ljubljana, Slovenia.

An  $(n_k)$  *combinatorial* configuration is a collection of  $n$  objects, called “points” and  $n$  collections of “points”, called “lines”, such that each point is incident with  $k$  lines and each line contains  $k$  points. Each combinatorial configuration is in one-to-one correspondence to a bipartite graph in which each point and each line corresponds to a node of the configuration and incident point- and line-nodes are connected by an edge of the graph; this incidence graph is called the *Levi graph* of the configuration. If the points are distinct points in some Euclidean space (usually the plane) and the lines are distinct straight lines, then we call this a *geometric* configuration, or a (*strong*) *geometric realization* of the corresponding combinatorial configuration.

A configuration is *self-dual* if there exists a color-exchanging automorphism of the corresponding Levi graph, which exchanges the roles of points and lines. We reserve the term “symmetry” to refer to the geometric symmetries of a particular geometric realization; for example, the realization of the Grünbaum–Rigby configuration shown in Figure 1(a) has seven-fold rotational symmetry.

A geometric configuration is *polycyclic* if the orbits of the points and lines under the action of the maximal rotational symmetry group each have the same number of elements; we call these orbits the *symmetry classes* of the configuration. A geometric configuration has a *polycyclic realization* if the corresponding semi-regular automorphism can be realized geometrically using  $k$ -fold rotational symmetry, where  $k$  is the order of the orbits of points and lines.

The study of polycyclic configurations was independently pursued and further developed by Grünbaum [16] as well as Berman and her coauthors DeOrsey, Faudree, Jaksch, Pisanski, Ver Hof and Žitnik (see, e.g. [2, 4, 5, 3]). It is closely intertwined with graph theory as well; for details on this connection, see [20].

In their paper, Grünbaum and Rigby conjectured:

1. that no other  $(21_4)$  configuration exists, and
2. no  $(n_4)$  configuration exists for  $n < 21$ .

It was a big surprise when Grünbaum himself disproved the second part of this conjecture [15] by constructing a  $(20_4)$  configuration, which we denote by  $G(20_4)$ . At that time, it was widely believed that the  $GR(21_4)$  configuration was the only geometric 4-configuration for  $n = 21$ , and that  $G(20_4)$  is the smallest geometric 4-configuration. However, a few years later, Bokowski and his coauthors Pilaud and Schewe showed that there are no  $(n_4)$  configurations for  $n \leq 17$ , that there are exactly two distinct  $(18_4)$  configurations [9, 10], and that no geometric  $(19_4)$  configuration exists [7].

A number of months ago, the first author of this paper constructed a new  $(21_4)$  geometric configuration, depicted in Figure 2, which provides a counterexample to the first part of the Grünbaum–Rigby conjecture. We denote this configuration by  $B(21_4)$ . The main goal of this paper is to provide a proof of existence of this configuration; we present both a synthetic and an analytic proof, since we believe that both have their benefits, and may form a suitable basis for extending the research to configurations with analogous structure. For the same reason, we also discuss some interesting structural properties of this configuration.

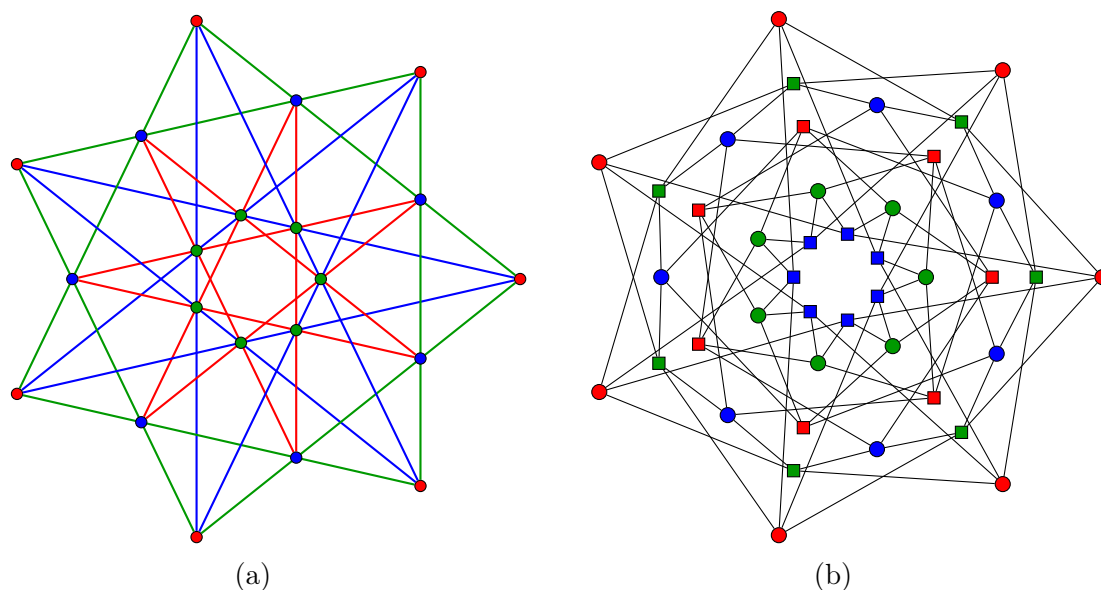


Figure 1: (a) The Grünbaum–Rigby (21<sub>4</sub>) geometric configuration, denoted by GR(21<sub>4</sub>), and (b) its Levi graph. In the Levi graph, point-vertices are shown with circles and line-vertices are shown with squares, and the colors correspond to the colors of the symmetry classes of the points and lines of the configuration. We note that the colors are also consistent with the self-dualities (in the sense that self-duality maps of the configuration preserve the colors; these maps correspond to certain automorphisms of the Levi graph).

## 2 A comparison of the configurations GR(21<sub>4</sub>) and B(21<sub>4</sub>)

It is not hard to verify that B(21<sub>4</sub>) is combinatorially distinct from GR(21<sub>4</sub>). Namely, one can compute the Levi graphs of both configurations. We used the computer algebra system *Sage* to prove that the two 4-valent graphs on 42 vertices are non-isomorphic. For instance, the Levi graph of B(21<sub>4</sub>) has only 12 automorphisms, while the Levi graph of GR(21<sub>4</sub>) has 672 automorphisms (including bipartition-reversing automorphisms, which correspond to self-dualities of these configurations).

The Levi graph of the Grünbaum–Rigby configuration, which we denote by L(GR), can be described as the Kronecker cover over the line graph of the renowned Heawood graph. Its automorphism group contains 672 elements. Half of them correspond to combinatorial self-dualities, while the other half correspond to combinatorial automorphisms of GR(21<sub>4</sub>). As for the latter, we know that the automorphism group of both the Heawood graph and the Grünbaum–Rigby configuration is **PGL**(2, 7) of order 336 [17], and is a subgroup of index 2 in the automorphism group of L(GR). We observe that out of the 336 combinatorial symmetries, only 14 are geometrically realizable in the standard polycyclic realization; also, from the 336 combinatorial self-dualities, 14 are geometrically realizable. This means that GR(21<sub>4</sub>) shown in Figure 1 geometrically realizes 28 out of the 672 graph automorphisms.

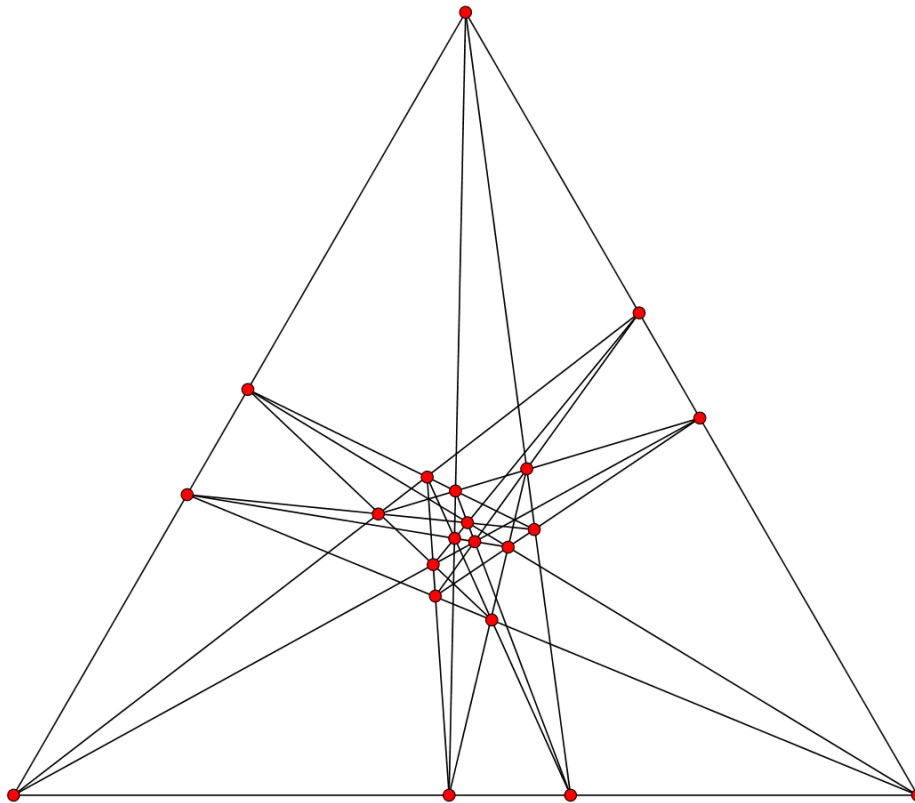


Figure 2: A new  $(21_4)$  geometric configuration, denoted by  $B(21_4)$ .

We used programs written in *Sage* to compute all semi-regular automorphisms of  $L(\text{GR})$  and the corresponding quotient graphs. The quotients that are bipartite correspond to *reduced Levi graphs*.

Here we recall that an automorphism  $\alpha$  of a graph  $G$  is called *semi-regular* if all of its orbits are of the same size, say  $k$ . It defines a projection  $\pi$  from  $G$  to the *quotient graph*  $B = G/\alpha$ ,  $\pi : G \rightarrow B = G/\alpha$ , that is a local isomorphism (also called *acovering projection*). By assigning arbitrarily directions to edges of  $B$ , and by an appropriate assignment of elements from  $\mathbb{Z}_k$  to the edges of  $G/\alpha$ , a *voltage graph* is obtained, and  $\mathbb{Z}_k$  is called the *voltage group*. A graph admitting a semi-regular automorphism  $\alpha$  is called *polycirculant* (with respect to  $\alpha$ ). Each quotient of a non-bipartite polycirculant graph is non-bipartite. However, a quotient of a bipartite polycirculant graph may be non-bipartite or bipartite. A bipartite quotient of a Levi graph is called a *reduced Levi graph* (RLG). The semi-regular automorphism producing an RLG has each orbit monochromatic. Each orbit corresponds either to a set of points or to a set of lines of the configuration. Reduced Levi graphs were introduced in Grünbaum's monograph [16]. There is a well-known procedure for reconstructing  $G$  from its voltage graph. For more details, see [16, 20, 2]). Here we only consider the case of RLGs.

Our computations show that there are 314 semi-regular automorphisms producing

8 distinct quotient graphs of  $L(\text{GR})$ . However, only two of them are bipartite, hence there exist only two non-isomorphic RLGs that can possibly correspond to polycyclic realizations of the Grünbaum–Rigby configuration.

The first RLG, on 6 vertices, is expected, since it can be deduced from Figure 1, and is depicted in Figure 3. The associated voltage group is  $\mathbb{Z}_7$ , consistent with the seven-fold rotational symmetry of the geometric Grünbaum–Rigby configuration.

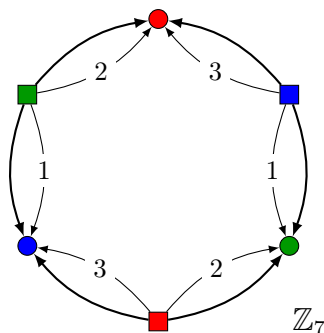


Figure 3: The reduced Levi graph  $\text{RLG}(\text{GR})$  with voltage group  $\mathbb{Z}_7$  for the polycyclic Grünbaum–Rigby  $\text{GR}(21_4)$  configuration with seven-fold rotational symmetry. The colors for the symmetry classes match the colors from Figure 1.

However, the second one, depicted in Figure 4a, was quite unexpected. It has 14 vertices, and the corresponding voltage group is  $\mathbb{Z}_3$ . Initially, we wanted to know if there existed a polycyclic geometric realization of the Grünbaum–Rigby configuration with three-fold rotational symmetry. All our attempts to generate such a realization based on the RLG shown in Figure 4a failed (see Section 6).

There is a simple algorithm that can produce a Levi graph from a reduced Levi graph. For a reduced Levi graph with voltage group  $\mathbb{Z}_m$ , the notation  $\boxed{L} \xrightarrow{a} \odot v$  means that there is a symmetry class of points labeled  $v$ , with elements  $v_i$ ,  $i = 0, \dots, m-1$ ; a symmetry class of lines  $L$ , with elements  $L_i$ ,  $i = 0, \dots, m-1$ ; and that each line  $L_i$  is incident with vertex  $v_{i+a}$ , with index arithmetic taken modulo  $m$ . For convenience, we provide an incidence table from the reduced Levi graph shown in Figure 4a, see Table 1.

### 3 A synthetic proof of the existence of $\text{B}(21_4)$

**Theorem 1.** *There exists a self-dual geometric, polycyclic  $(21_4)$  configuration with three-fold rotational symmetry.*

Here we recall that a configuration  $\mathcal{C}$  is called *self-dual* if there is an incidence-preserving correspondence that maps the points of  $\mathcal{C}$  onto its lines and vice versa [16, 20]. (Note that this is equivalent to the definition given in the Introduction.)

Before proving this theorem, we need some more preliminaries.

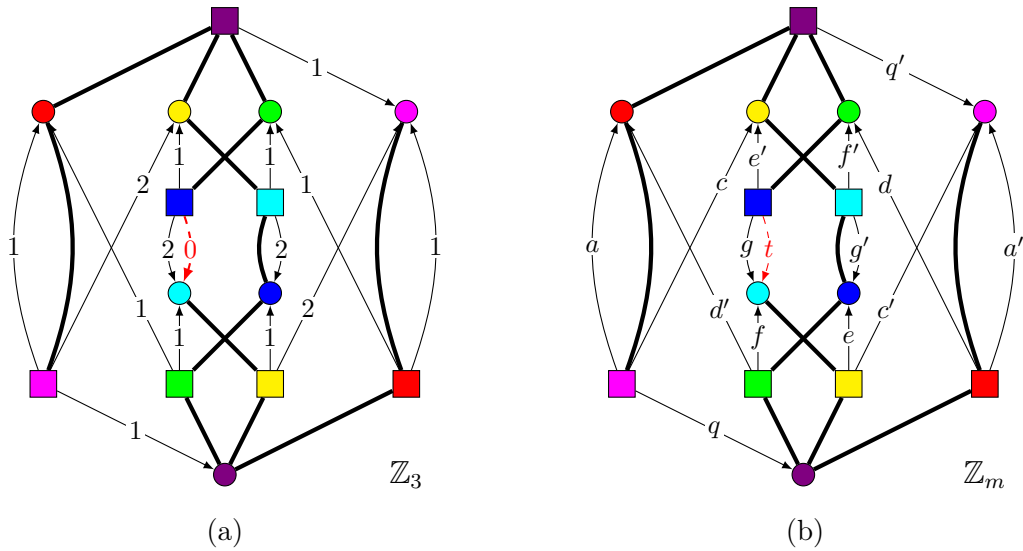


Figure 4: (a) The reduced Levi graph  $\text{RLG}(B)$  for the configuration  $B(21_4)$ . The voltage group is  $\mathbb{Z}_3$ , expressing the fact that this configuration exhibits three-fold rotational symmetry. Point orbits of  $B(21_4)$  are represented by circular nodes and line orbits by rectangular nodes. The color-preserving rotational symmetry of order two of the graph corresponds to a self-duality of the configuration. (b) A version of the RLG with generic parameters.

$r_0$	$M_0$	$M_1$	$G_1$	$P_0$	$r_1$	$M_1$	$M_2$	$G_2$	$P_1$	$r_2$	$M_2$	$M_0$	$G_0$	$P_2$
$y_0$	$M_2$	$B_1$	$C_0$	$P_0$	$y_1$	$M_0$	$B_2$	$C_1$	$P_1$	$y_2$	$M_1$	$B_0$	$C_2$	$P_2$
$g_0$	$B_0$	$C_1$	$R_1$	$P_0$	$g_1$	$B_1$	$C_2$	$R_2$	$P_1$	$g_2$	$B_2$	$C_0$	$R_0$	$P_2$
$m_0$	$Y_2$	$R_0$	$R_1$	$P_1$	$m_1$	$Y_0$	$R_1$	$R_2$	$P_2$	$m_2$	$Y_1$	$R_2$	$R_0$	$P_0$
$b_0$	$C_0$	$C_2$	$Y_1$	$G_0$	$b_1$	$C_1$	$C_0$	$Y_2$	$G_1$	$b_2$	$C_2$	$C_1$	$Y_0$	$G_2$
$c_0$	$B_0$	$B_2$	$G_1$	$Y_0$	$c_1$	$B_1$	$B_0$	$G_2$	$Y_1$	$c_2$	$B_2$	$B_1$	$G_0$	$Y_2$
$p_0$	$R_0$	$Y_0$	$G_0$	$M_1$	$p_1$	$R_1$	$Y_1$	$G_1$	$M_2$	$p_2$	$R_2$	$Y_2$	$G_2$	$M_0$

Table 1: The incidence table of  $B(21_4)$ .

### 3.1 Quasi-configurations

Recall that an *incidence structure*  $\mathcal{C}$  is a triple  $\mathcal{C} = (P, B, I)$ , where  $P$  is the set of *points*,  $B$  is the set of *lines* (or *blocks*), and  $I \subseteq P \times B$  is the *incidence relation* [20]. Given an incidence structure  $\mathcal{C} = (P, B, I)$ , assume that  $P$  is a disjoint union of subsets  $P_i$  of cardinality  $p^i$  ( $i = 1, 2, \dots, m(P)$ ), and  $L$  is a disjoint union of subsets  $L_j$  of cardinality  $n^j$  ( $j = 1, 2, \dots, m(L)$ ). We call  $\mathcal{C}$  a (combinatorial) *quasi-configuration of type*

$$((p_{q_1}^1)(p_{q_2}^2) \dots (p_{q_m(P)}^{m(P)}), (n_{k_1}^1)(n_{k_2}^2) \dots (n_{k_m(L)}^{m(L)})),$$

if each point in  $P_i$  is incident with  $q_i$  lines, and each line in  $L_j$  is incident with  $k_j$  points. (We note that here we adopt the term used by Bokowski and Pilaud [8], but with slightly different meaning.)

Observe that a quasi-configuration with  $m(P) = m(L) = 1$  is a configuration in the usual sense. In analogy with the case of configurations, if all the numerical parameters of a quasi-configuration  $\mathcal{C}$  are the same for the points and the lines, we use the simplified notation

$$((n_{k_1}^1)(n_{k_2}^2) \dots (n_{k_{m(L)}}^{m(L)})),$$

and we say that  $\mathcal{C}$  is *balanced* (here we adopt the term introduced by Grünbaum [16]). In particular, below we construct a quasi-configuration of type  $((6_2)(9_4))$ , where the type notation shows that it contains

- 6 points, each incident to 2 lines,
- 9 points, each incident to 4 lines, and conversely,
- 6 lines, each incident to 2 points and
- 9 lines, each incident to 4 points.

### 3.2 Self-reciprocity

It is clear that the notions of duality and self-duality of configurations applies also to quasi-configurations. In particular, it is also clear that a self-dual quasi-configuration is necessarily balanced. A stronger version of duality is when it is induced by reciprocation with respect to a circle. (We note that, in general, reciprocation with respect to a circle is a useful tool for producing the dual of a configuration [16]; it is a simple procedure which means constructing the polar in the case where the conic of polarity is a circle.) We say that a quasi-configuration  $\mathcal{C}$  is *self-reciprocal* if there is a circle  $\Omega$  such that the reciprocation with respect to  $\Omega$  sends  $\mathcal{C}$  to its isometric copy. We distinguish three particular cases of self-reciprocity. We call  $\mathcal{C}$  *perfectly self-reciprocal* if it coincides with its reciprocal. The Grünbaum–Rigby configuration provides an example of a perfectly self-reciprocal configuration (further examples occur in [14], where this notion is applied for the first time). Two slightly weaker versions are when for attaining coincidence one has to apply a subsequent rotation or reflection on the reciprocal image. In these cases we speak of a *rotationally* or *reflexibly self-reciprocal* configuration, respectively. Figure 5 shows an example of a polycyclic  $(24_4)$  configuration which is rotationally self-reciprocal. One directly observes that, in addition, it is mirror symmetric (with 12 mirror lines); this implies that it is reflexibly self-reciprocal as well. We remark that Branko Grünbaum in his book [16] uses the term *oppositely self-polar* for a configuration with this latter property; in his Figure 5.8.2 he presents precisely this configuration for an example.

Given a polycyclic (quasi-)configuration  $\mathcal{C}$  realized with  $k$ -fold rotational symmetry possessing any of the self-reciprocity properties mentioned above, any (say, the  $i$ th) orbit of points with respect to  $\mathbb{Z}_k$  is located on a circle  $\Gamma_i$  concentric with  $\Omega$ ; furthermore,

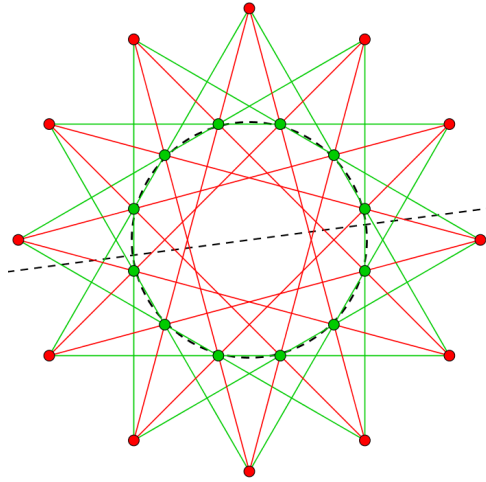


Figure 5: Example of a configuration which is both rotationally and reflexibly self-reciprocal. The circle of reciprocity is shown by dashed line. The angle of rotation for attaining coincidence is  $\pi/12$ . The reciprocal image will also coincide with the original copy by reflecting it in the mirror line shown dashed (there are 12 such mirror lines).

the orbit of the corresponding polar lines has an incircle  $\Gamma'_i$  (also concentric with  $\Omega$ ). Obviously,  $\Gamma_i$  and  $\Gamma'_i$  are inverse images of each other with respect to  $\Omega$ , in other words,  $\Omega$  is the *midcircle* of these circles.

The mid-circle can be constructed in the following way. Take a ray starting from the common center  $O$ , and let it intersect  $\Gamma_i$  and  $\Gamma'_i$  in points  $P$  and  $P'$ , respectively. Take the Thales' circle  $\mathcal{T}$  with diameter  $PP'$ , and construct a tangent line to  $\mathcal{T}$  from the point  $O$ . Let  $T$  be the point of tangency. Then the midcircle is obtained as a circle of radius  $OT$  centered at  $O$ . We recall that this construction is based on some elementary properties of inversion with respect to a circle [11], which can be summarized in the following proposition.

**Proposition 2.** *Let  $\Omega$  be the circle of an inversion  $\varphi$ , and let  $\Gamma_1$  be a circle. Then the following conditions are equivalent.*

1.  $\Gamma_1$  is invariant under  $\varphi$ ;
2. if  $\Gamma_1$  passes through a point  $P$ , then it also passes through  $\varphi(P)$ ;
3.  $\Gamma_1$  is orthogonal to  $\Omega$ .

### 3.3 A quasi-configuration of type $((6_2)(9_4))$

Before stating our proposition here, we recall that (following Grünbaum [16]) a configuration is called *rigid* if its geometric realizations form a single class under projective transformations. We say that it is *movable* if it has more than one projectively non-equivalent realization; that is, if four points of the configuration in general position can



be fixed and a fifth point can be moved while maintaining incidence. Accordingly, given a movable configuration  $\mathcal{C}$ , the number of parameters that can be changed independently when moving  $\mathcal{C}$  is called the degree of freedom.

**Proposition 3.** *There exists a self-reciprocal quasi-configuration of type  $((6_2)(9_4))$  with three-fold rotational symmetry. It is movable, with one degree of freedom.*

We denote this quasi-configuration by  $\text{QC}(\text{B})$ . It is depicted in Figure 6. We distinguish the orbits of points and lines (w.r.t. its rotational symmetry group) by colors, namely, we use green, magenta, purple, red and yellow. The points and lines will be denoted accordingly by  $X_i$  and  $x_i$  ( $i = 0, 1, 2$ ), respectively, where  $X$  and  $x$  is the initial of the name of the corresponding color. The corresponding orbit of points and lines will be denoted by  $(X)$  and  $(x)$ , respectively. As we shall see below, this quasi-configuration forms a substructure of  $\text{B}(21_4)$ ; hence here we use for labelling its points and lines the labels taken from Table 1.

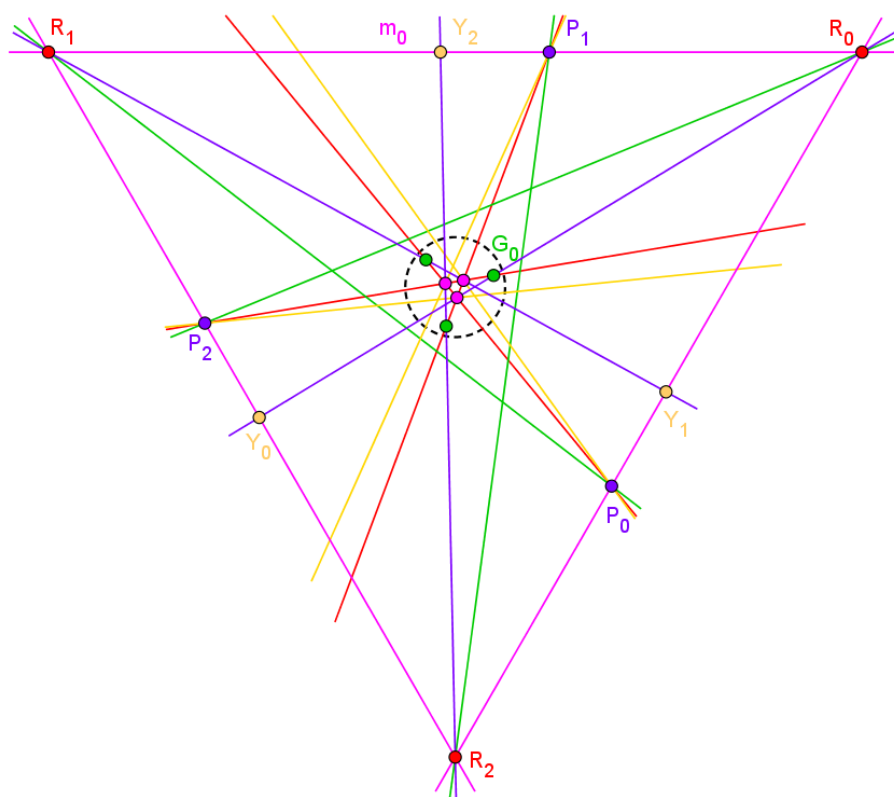


Figure 6: The quasi-configuration  $\text{QC}(\text{B})$ . The circle of reciprocity is also shown (drawn dashed).

*Remark 4.* Throughout the construction given in the proof below, the indices are meant modulo 3. In addition, we use the convention that rotation either of a point  $X_i$  or of a line  $x_i$  by angle  $+120^\circ$  (i.e., counterclockwise) increases  $i$  by one; the center of rotation coincides with center  $O$  of the triangle  $R_0R_1R_2$ .

*Proof.* We give a construction for QC(B) in the following 11 steps.

1. Fix an equilateral triangle with red vertices  $R_i$  and magenta side lines  $m_i = R_i R_{i+1}$ .
2. Take a yellow point  $Y_2$  on the line  $m_0$  such that it can be shifted freely in the interior of the segment  $\overline{R_1 M_{01}}$ , where  $M_{01}$  denotes the midpoint of the side  $R_0 R_1$  of the triangle  $R_0 R_1 R_2$ . Take also the rotates of this point by angle  $\pm 120^\circ$ .
3. Take the purple line  $p_2 := Y_2 R_2$  and its corresponding rotates.
4. Let  $A$  be an auxiliary point defined as the intersection  $A := \overline{Y_0 Y_1} \cap \mathcal{C}(R_1 O R_2)$ , where  $\overline{Y_0 Y_1}$  is the segment connecting  $Y_0$  and  $Y_1$ , and  $\mathcal{C}(R_1 O R_2)$  is an auxiliary circle circumscribed on the points  $R_1, R_2$  and the center  $O$ .
5. Take the green line  $g_1 := R_2 A$  and its corresponding rotates.
6. Take the purple point of intersection  $P_0 := g_0 \cap m_2$ , and its rotates  $P_1$  and  $P_2$ .
7. Take the circumcircle of the points  $P_0, P_1, P_2$ , and the incircle of the triangle formed by the lines  $p_0, p_1, p_2$ . Construct the mid-circle of these circles; denote it by  $\Omega$ .
8. Take the circumcircle  $\gamma_R$  of the points  $R_0, R_1, R_2$ , and invert it in the circle  $\Omega$ . Denote the inverse circle by  $\gamma_r$ . Draw tangents to  $\gamma_r$  from the point  $P_1$ , and choose the one subtending the smaller angle with the line  $g_1$ . Let it be a red line denoted by  $r_1$ ; take its corresponding rotates  $r_2$  and  $r_0$ .
9. Take the point of intersection  $G_0 := p_0 \cap r_2$ , and its rotates.
10. Take the circumcircle  $\gamma_Y$  of the points  $Y_0, Y_1, Y_2$ , and invert it in the circle  $\Omega$ . Denote the inverse circle by  $\gamma_y$ . Draw tangents to  $\gamma_y$  from the point  $P_1$ , and choose the one subtending the greater angle with the line  $g_1$ . Let it be a yellow line denoted by  $y_1$ ; take its corresponding rotates  $y_2$  and  $y_0$ .
11. Take the point of intersection  $M_0 := p_2 \cap r_2$ , and its rotates.

The construction of QC(B) is thus complete. It is directly seen that this structure is *movable*: indeed, it can be transformed into infinitely many projectively inequivalent versions while preserving incidences, by shifting the point  $Y_2$  on the line  $m_0$  (within the interval  $R_1 M_{01}$ , as determined in step (2)). Thus, the degree of freedom is 1; using the auxiliary elements in step (4) serves the very purpose of preventing larger degree of freedom from appearing.

By an easy check one sees that each point has its dual counterpart and vice versa. The duality is induced by reciprocation with respect to the circle  $\Omega$  constructed in step (7); thus, duality  $(P) \leftrightarrow (p)$  is defined there. The orbit  $(r)$  is defined in step (8) using the same reciprocation, thus duality  $(R) \leftrightarrow (r)$  also holds. Similarly, step (10) defines duality  $(Y) \leftrightarrow (y)$ . By comparing the definition of orbit  $(G)$  in step (9) with the definition and

a property of orbit  $(g)$  in steps (5) and (6), and using the already established dualities, one sees that duality  $(G) \leftrightarrow (g)$  holds as well. Finally, duality  $(M) \leftrightarrow (m)$  can be verified similarly by a comparison of steps (1) and (11). Observe that coloring the points and lines indicates their duality.

From the type  $((6_2)(9_4))$  of  $QC(B)$  one obtains that there are 48 incidences; due to symmetry, this means 16 incidence types, i.e. combinations of colors of the form  $(X, x')$ . From Figure 6 one can see that because of the presence of two trilaterals (with red vertices and with magenta vertices) this number reduces to 14. 13 types of incidences are defined directly in the construction; in the order of occurrence, these are:  $(R, m)$ ,  $(Y, m)$ ,  $(R, p)$ ,  $(Y, p)$ ,  $(R, g)$ ,  $(P, g)$ ,  $(P, m)$ ,  $(P, r)$ ,  $(G, p)$ ,  $(G, r)$ ,  $(P, y)$ ,  $(M, p)$ ,  $(M, r)$ . One observes that by the definition of the points and lines, and their duality established above, 12 of these incidences can be ordered into 6 dual pairs of the form  $((X, x'), (X', x))$ . Finally, the last, 13th incidence  $(M, y)$  also holds, which is verified by duality since we have  $(Y, m)$ .  $\square$

### 3.4 Proof of Theorem 1

*Proof of Theorem 1.* Here we continue the construction given above with additional steps.

12. Define  $B_0$  as the point of intersection  $B_0 := g_0 \cap y_2$ , and similarly its rotates by cyclic permutation of the indices.
13. Define the cyan line  $c_0 := B_0 B_2$ , and similarly its rotates by cyclic permutation of the indices.
14. Take the circumcircle  $\gamma_B$  of the blue points  $B_0, B_1, B_2$ , and invert it with respect to the circle  $\Omega$ . Denote the resulted circle by  $\gamma_b$ . Draw tangents to this circle from the point  $Y_2$ , and choose the one that is separated from the center  $O$  by the line  $p_2$ . Denote it  $b_1$ , and take its rotates  $b_2$  and  $b_0$ .
15. Define  $C_0$  as the point of intersection  $C_0 := b_0 \cap b_1$ , and similarly its rotates by cyclic permutation of the indices.
16. Take the point of intersection of  $c_1$  and  $m_0$ , and denote it by  $Y'_2$ .

Observe that the incidence structure obtained in steps 1–16 above is movable. In fact,  $QC(B)$  is movable, as we have seen in the preceding subsection, and this property has been preserved throughout the additional steps 12–16. In the following, we utilize this property. Indeed, consider the mutual position of the points  $Y_2$  and  $Y'_2$  within the interval  $(R_1 M_{01})$ .

17. Move  $Y_2$  along the given interval.

Now, one observes that while shifting  $Y_2$  along this interval,  $Y'_2$  moves in the opposite direction. In particular, both cases of the order of the following four points may occur, such as  $(R_1, Y'_2, Y_2, M_{01})$  and  $(R_1, Y_2, Y'_2, M_{01})$  (this is checked in a dynamic geometry model). Hence, by continuity, an intermediate case must exist, where  $Y_2$  and  $Y'_2$  will

coincide. This is precisely the case where our movable structure obtained above becomes equal to  $B(21_4)$ .

This continuity argument is justified by the following observation. When building the incidence structure through steps (1–16), in each step where a new point or line is defined, its position is a continuous function of that of the already existing geometric constituents used in the definition. This is in fact a simple observation, provided we restrict ourselves to the domain  $(R_1M_{01})$ , where the first movable point  $Y_2$  is located.

Now we check the new incidences which occurred in this second part of our construction. Incidences  $(B, g)$ ,  $(B, y)$  and  $(B, c)$  exist by definition. Since orbit  $(b)$  is defined by reciprocating  $(B)$ , the dual incidences  $(G, b)$ ,  $(Y, b)$  also hold. Again, we have  $(C, b)$  by definition. It follows the triangles  $B_0B_1B_2$  and  $C_0C_1C_2$  are dual to each other (by reciprocating in  $\Omega$ ). This means, in particular, that orbits  $(C)$  and  $(c)$  are dual to each other. From the continuity argument we infer that incidence  $(Y, c)$  holds. By duality,  $(C, y)$  also holds.

What remain to be verified are incidences  $(C, g)$  and  $(G, c)$ ; in fact, either of them is sufficient by duality. We choose  $(C, g)$ . For illustration, we use Figure 7.

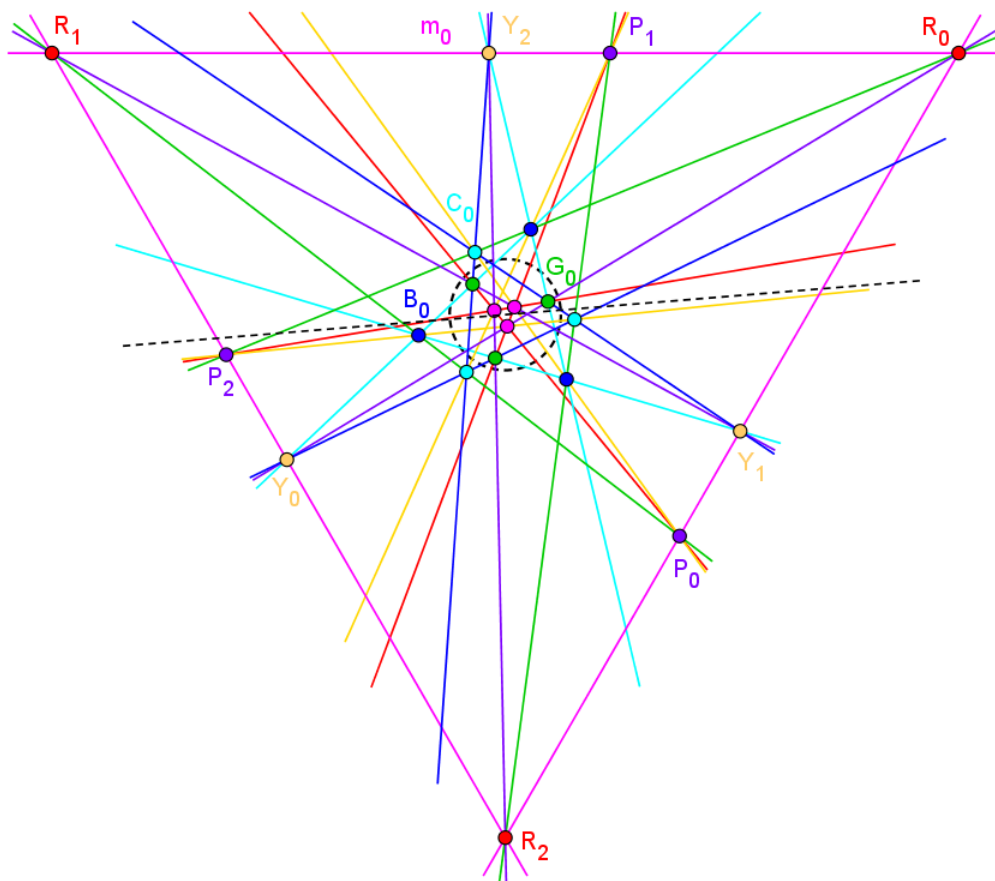


Figure 7: The configuration  $B(21_4)$  with the circle of reciprocation indicated. The mirror line belonging to the self-reciprocation  $\mathbf{d}$  given in Section 4 is also shown by a dashed line.

Draw the auxiliary circle  $\Gamma_a$  through the points  $Y_0$ ,  $O$ ,  $R_1$ . Due to the rotational symmetry, the angles  $R_0Y_2O$  and  $R_1Y_0O$  are equal. On the other hand, the angles  $R_0Y_2O$  and  $OY_2R_1$  are supplementary, thus so are the angles  $OY_2R_1$  and  $R_1Y_0O$ . Hence the quadrangle  $R_1Y_0OY_2$  is cyclic, which means that its vertex  $Y_2$  also lies on the circumference of  $\Gamma_a$ .

Since its angle at vertex  $R_1$  is  $60^\circ$ , the angle at the opposite vertex  $O$  is  $120^\circ$ . Observe that this latter angle is subtended by the arc  $Y_2R_1Y_0$ . In addition, the angle  $Y_0C_1Y_2$  is subtended by the same arc, and (since it is the point of intersection of two blue lines) it is also  $120^\circ$ ; hence its vertex  $C_1$  lies on the circumference of  $\Gamma_a$ .

Consider now the angles  $OR_1C_1$  and  $OY_2C_1$ . Since they are subtended by the same arc (determined by  $C_1$  and  $O$ ), while their vertex  $R_1$  resp.  $Y_2$  lie on the circumference of  $\Gamma_a$ , they are equal. Take the vertices of the triangle determined by the green lines, and denote them by  $U_0$ ,  $U_1$  and  $U_2$ . Observe that the line  $OU_1$  bisects the angle at  $U_1$  of the triangle  $U_0U_1U_2$ , and so does the line  $OR_1$  the angle at  $R_1$  of the triangle  $R_0R_1R_2$ ; hence both of these angles are  $30^\circ$ . It follows that the triangles  $OR_1U_1$  and  $OY_2C_1$  are similar to each other (these triangles are highlighted in Figure 8 by red and yellow, respectively).

Recall that by a basic theorem of Euclidean plane geometry, any two similar triangles  $A_1A_2A_3$  and  $A'_1A'_2A'_3$  determine a unique similarity transformation which sends the vertex  $A_i$  to vertex  $A'_i$  for all  $i \in \{1, 2, 3\}$ . If the triangles are oriented alike, then this transformation is a dilative rotation [12]. In our case, we see that we have a dilative rotation  $\varrho$  such that its fixed point is the common vertex  $O$  of the red and yellow triangle considered above, and it acts on the two other vertices as follows:

$$\varrho : R_1 \mapsto Y_2, U_1 \mapsto C_1.$$

Taking into account the three-fold rotational symmetry, we see that  $\varrho$  transforms the equilateral triangle  $R_0R_1R_2$  into the triangle  $Y_1Y_2Y_0$  inscribed in it (in the sense that the vertices of the latter are incident to the side lines of the former). Thus we conclude that  $\varrho$  acts on the triangle  $U_0U_1U_2$  in the same way, which means that this triangle is transformed into the triangle whose side lines are the blue lines, vertices are the cyan points, moreover, it is inscribed in the triangle  $U_0U_1U_2$ . But the side lines of the triangle  $U_0U_1U_2$  are the green lines, hence we see that the incidence  $(C, g)$  holds indeed.  $\square$

Based on the construction above, here we provide the coordinates of the initial four points determining the configuration. Assume that the red points are located as follows:

$$R_0 = (\sin(120^\circ), 0.5); \quad R_1 = (\sin(-120^\circ), 0.5); \quad R_2 = (0, -1).$$

Then  $Y_2$  can be given (up to 15 decimals) as follows:

$$Y_2 = (-0.031440363334572, 0.5).$$

## 4 Automorphisms and self-dualities of $B(21_4)$

We denote the automorphism group of the Levi graph of  $B(21_4)$  by  $\text{Aut } L(B)$ . By our programs written in *Sage* (mentioned in Section 2) we know that it is isomorphic to the dihedral group  $D_6$  of order 12 (see item 1 in Table 2).

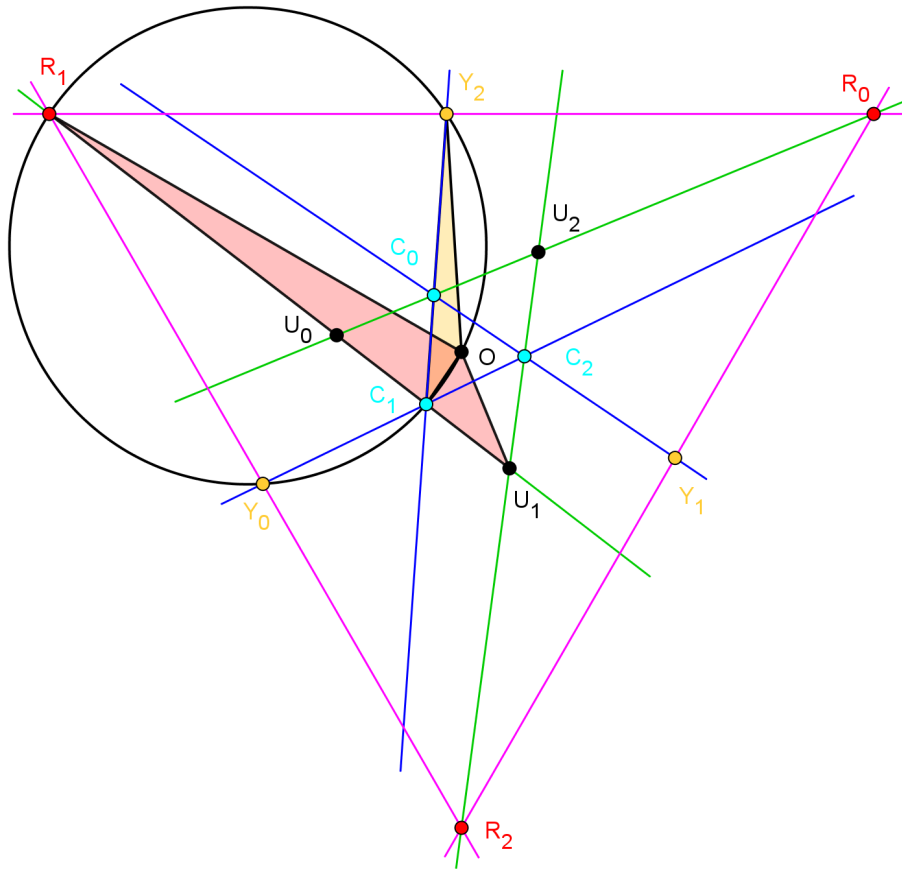


Figure 8: Illustration for the verification of incidence  $(C, g)$ .

It is generated by two generators  $\mathbf{r}, \mathbf{d}$  such that it is given by the following presentation:

$$\langle \mathbf{r}, \mathbf{d} \mid \mathbf{r}^6 = \mathbf{d}^2 = (\mathbf{r}\mathbf{d})^2 = \mathbf{1} \rangle. \quad (1)$$

The corresponding Cayley graph of this group is depicted in Figure 9.

In our case, the generators take the following form:

$$\begin{aligned} \mathbf{r} = & (R_0, M_0, R_1, M_1, R_2, M_2)(Y_0, G_2, Y_1, G_0, Y_2, G_1) \\ & (B_0, C_2, B_1, C_0, B_2, C_1)(P_0, P_2, P_1) \\ & (r_0, m_1, r_1, m_2, r_2, m_0)(y_0, g_2, y_1, g_0, y_2, g_1) \\ & (b_0, c_2, b_1, c_0, b_2, c_1)(p_0, p_2, p_1), \end{aligned} \quad (2)$$

$$\mathbf{d} = (R_0, r_1)(R_1, r_0)(R_2, r_2)(Y_0, y_1)(Y_1, y_0)(Y_2, y_2) \\ (P_0, p_1)(P_1, p_0)(P_2, p_2)(G_0, g_1)(G_1, g_0)(G_2, g_2) \\ (B_0, b_1)(B_1, b_0)(B_2, b_2)(C_0, c_1)(C_1, c_0)(C_2, c_2) \\ (M_0, m_1)(M_1, m_0)(M_2, m_2). \quad (3)$$

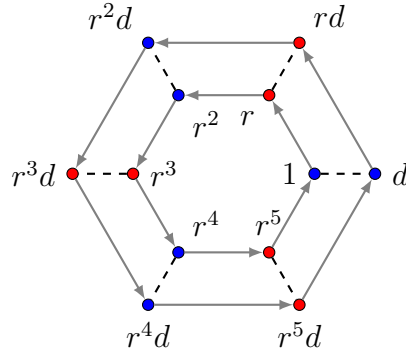


Figure 9: The Cayley graph of  $\text{Aut } L(B)$  corresponding to the presentation (1); the generator  $\mathbf{r}$  is shown with gray arrows and the involutory generator  $\mathbf{d}$  with dashed edges. The red vertices represent purely combinatorial automorphisms which cannot be realized geometrically (that is, using reciprocation and reflections or rotations).

Using Table 1 one can directly check that  $\mathbf{r}$  and  $\mathbf{d}$  are indeed Levi graph automorphisms that generate the whole automorphism group of order 12.

On the other hand, taken to the second power

$$\begin{aligned} \mathbf{r}^2 = & (R_0, R_1, R_2)(r_0, r_1, r_2)(Y_0, Y_1, Y_2)(y_0, y_1, y_2)(P_0, P_1, P_2)(p_0, p_1, p_2) \\ & (G_0, G_1, G_2)(g_0, g_1, g_2)(B_0, B_1, B_2)(b_0, b_1, b_2)(C_0, C_1, C_2)(c_0, c_1, c_2) \\ & (M_0, M_1, M_2)(m_0, m_1, m_2), \end{aligned} \quad (4)$$

one obtains a (geometric) rotation of order 3, which generates the symmetry group  $\text{Sym } B(21_4) = \langle \mathbf{r}^2 \rangle \cong \mathbb{Z}_3$  of  $B(21_4)$ . We note that this verifies as well that  $B(21_4)$  is a polycyclic configuration with respect to  $\mathbb{Z}_3$ .

The automorphism  $\mathbf{r}$  generates the full automorphism group  $\text{Aut } B(21_4) \cong \mathbb{Z}_6$  of our configuration. The other 6 elements of  $\text{Aut } L(B)$  are all (involutory) self-dualities of  $B(21_4)$ . Three of them are purely combinatorial self-dualities (see Figure 9). On the other hand,  $\mathbf{d}$  given by equality (3), and its two conjugates  $\mathbf{r}^2\mathbf{d}$  and  $\mathbf{r}^4\mathbf{d}$  are realized as geometric transformations. Namely, they are reflexible self-reciprocations of  $B(21_4)$ . The circle of reciprocation is shown in Figure 7. The mirror line belonging to  $\mathbf{d}$  is also shown in the same figure; the mirror lines belonging to the two other self-reciprocations are rotates of this line by angles  $\pm 120^\circ$ .

As it can directly be seen from Figure 9, one of the purely combinatorial self-dualities is given as  $\mathbf{r}^5\mathbf{d} = \mathbf{d}\mathbf{r}$ . Using equalities (2) and (3), for this product one obtains the following expression:

$$\begin{aligned} \mathbf{d}\mathbf{r} = & (R_0, m_2)(R_1, m_1)(R_2, m_0)(Y_0, g_0)(Y_1, g_2)(Y_2, g_1) \\ & (P_0, p_0)(P_1, p_2)(P_2, p_1)(G_0, y_0)(G_1, y_2)(G_2, y_1) \\ & (B_0, c_0)(B_1, c_2)(B_2, c_1)(C_0, b_0)(C_1, b_2)(C_2, b_1) \\ & (M_0, r_1)(M_1, r_0)(M_2, r_2). \end{aligned} \quad (5)$$

Observe that the symmetry properties of the reduced Levi graph of  $B(21_4)$  show both types of self-duality: indeed, its half-turn symmetry (i.e. rotational symmetry of order two) shows self-reciprocity, while the mirror symmetry with respect to a horizontal axis shows precisely the type of combinatorial duality given by the expression above (see the colors of the nodes representing the point orbits and line orbits of the configuration).

We conclude this subsection with some questions related to the rank of self-duality. Let  $\mathcal{C}$  be a self-dual configuration, and let  $\delta$  denote a self-duality map of  $\mathcal{C}$ . The *rank*  $r(\delta)$  of  $\delta$  is defined as its order, i.e. the smallest positive integer  $n$  such that  $\delta^n$  is the identity. A configuration may have more than one self-duality maps (in our case we have altogether 6, as we have seen above), thus the following definition makes sense. The *rank*  $r(\mathcal{C})$  of a self-dual configuration  $\mathcal{C}$  is the minimum value of  $r(\delta)$  over all self-duality maps  $\delta$  of  $\mathcal{C}$ . (We note that this notion was introduced by Grünbaum and Shephard [18] in case of geometric objects for which self-duality can be defined, in particular, for polyhedra and configurations; for further details related to configurations, see [16] and the references therein).

As we have seen above, all the self-dualities of  $B(21_4)$  are involutory, thus its rank  $r(B(21_4)) = 2$ . But as we have also seen,  $B(21_4)$  is reflexibly self-reciprocal; hence the question arises that, in general, does the latter property imply the former? It is appropriate here to cite a conjecture by Grünbaum [16, Conjecture 5.8.1].

**Conjecture 5.** Every self-dual geometric configuration of rank 2 has a realization such that its polar (in a suitable circle) is congruent to the original configuration.

(We note that “congruent” is meant here in the usual geometric sense, i.e. two geometric configurations are called congruent if there is an isometry of the ambient space that maps the one into the other.)

## 5 Analytic proof of the existence of the configuration $B(21_4)$

We use the reduced Levi graph shown in Figure 4a as a “recipe” to construct the configuration analytically with homogeneous coordinates, using *Mathematica*. We are interested in constructing a strong realization of the configuration, in which all the points and lines are distinct.

There are a number of ways to walk through the reduced Levi graph. Here, we present one which uses only meets and joins so that in the final steps, we are solving a system of two polynomials in two unknowns. We begin by fixing the red points and magenta lines. (For convenience, we use a rotated starting position for the red points from that used in the previous section.) We make the following assignments, following the labels on the reduced Levi graph shown in Figure 4b with the assignments from Figure 4a.

$$\{a, c, d, e, f, g, q, a', c', d', e', f', g', q', t\} = \{1, 2, 1, 1, 1, 2, 1, 1, 2, 1, 1, 1, 2, 1, 0\}.$$

We place a yellow point  $Y_i$  arbitrarily (using parameter  $x$ ) on a magenta line  $m_{i-a}$ , and then use the red points  $R_i$  and yellow points  $Y_i$  to define the purple lines  $p_i$ . On the purple



line  $p_i$ , we place a green point  $G_i$  arbitrarily, using parameter  $z$ . The rest of the points and lines are determined, as follows, in order (all indices taken mod 3):

$$\begin{aligned}
R_i &= (2 \cos(2\pi i/3), 2 \sin(2\pi i/3), 1) \\
m_i &= R_i \times R_{i+a} \\
Y_i &= (1-x)m_{i-c} + xm_{i-c+a} \\
p_i &= Y_i \times R_i \\
G_i &= (1-z)R_i + zY_i \\
b_i &= Y_{i+e'} \times G_i \\
c_i &= Y_i \times G_{i+f'} \\
C_i &= b_{i-g} \times b_{i-t} \\
B_i &= c_{i-g'} \times c_i \\
g_i &= C_{i+f} \times B_i \\
y_i &= C_i \times B_{i+e} \\
M_i &= y_{i-c'} \times p_{i-q'} \\
r_i &= G_{i+d} \times M_i.
\end{aligned} \tag{6}$$

As we made these assignments, we eliminated any common numeric or polynomial factors from the homogeneous coordinates. After these simplifications, we computed two determinants: the reduced Levi graph says that we need  $R_{d'}, C_f, B_0$  collinear (on  $g_0$ ) and  $M_0, M_{a'}, G_d$  collinear (on  $r_0$ ). Define

$$\begin{aligned}
\text{det1} &= \det(R_{d'} \ C_f \ B_0) \\
&= -6\sqrt{3}(x-1)z(2x^2z+x^2-2xz-x+z)(3x^3z-x^2z^2-4x^2z-x^2+xz^2+3xz-z^2)
\end{aligned}$$

and

$$\begin{aligned}
\text{det5} &= \det(M_0 \ M_{a'} \ G_d) \\
&= 6\sqrt{3}(x^2z-xz-x+z)(2x^2z+x^2-2xz-x+z)(3x^6z^3+6x^6z^2-7x^5z^3 \\
&\quad -27x^5z^2-2x^5+9x^4z^3+53x^4z^2-9x^4z+7x^4-6x^3z^3-62x^3z^2 \\
&\quad +25x^3z-11x^3+2x^2z^3+44x^2z^2-28x^2z+10x^2-18xz^2+15xz-5x \\
&\quad +3z^2-3z+1)
\end{aligned}$$

These two determinants have a common factor

$$\text{common} = 6\sqrt{3}(2x^2z+x^2-2xz-x+z);$$

solving  $\text{common} = 0$  for  $z$  in terms of  $x$  yields

$$z = \frac{x-x^2}{2x^2-2x+1}. \tag{7}$$

Performing this substitution into both  $M_{-q'}$  and  $Y_0$ , for example, which both lie on the purple line  $p_0$ , shows that the two points coincide, which is forbidden in a strong realization of the reduced Levi graph.

Reducing the two determinants into  $\det 1'$  and  $\det 5'$  respectively by eliminating the common factor and solving the associated system

$$\{\det 1' = 0, \det 5' = 0\} \quad (8)$$

over  $\mathbb{R}$  results in a collection of solutions. Some of the solutions are degenerate,

$$\{\{x \rightarrow 0, z \rightarrow 0\}, \left\{x \rightarrow \frac{1}{2}, z \rightarrow 0\right\}, \left\{x \rightarrow \frac{1}{2}, z \rightarrow \frac{2}{3}\right\}, \{x \rightarrow 1, z \rightarrow 0\}, \{x \rightarrow 1, z \rightarrow 1\},$$

because these all immediately lead to coinciding points in the construction.

However, there are exactly two non-degenerate solutions over  $\mathbb{R}$ , which *Mathematica* can express exactly as roots of certain polynomials with integer coefficients: let

$$\begin{aligned} \alpha(s) &= 9s^{12} - 45s^{11} + 108s^{10} - 114s^9 - 57s^8 + \\ &\quad 390s^7 - 668s^6 + 684s^5 - 468s^4 + 217s^3 - 66s^2 + 12s - 1 \\ \beta(s) &= s^{12} + 9s^{11} + 15s^{10} - 36s^9 - 33s^8 + \\ &\quad 129s^7 - 193s^6 + 216s^5 - 162s^4 + 76s^3 - 24s^2 + 6s - 1 \end{aligned}$$

Both of these polynomials have exactly two real roots. The two solutions  $(x, z)$  to (8) are

$$\begin{aligned} x &= \text{Root}(\alpha(s), 1) \approx -1.66271 \\ z &= \text{Root}(\beta(s), 1) \approx -5.40326 \end{aligned}$$

and

$$\begin{aligned} x &= \text{Root}(\alpha(s), 2) \approx 0.518152 \\ z &= \text{Root}(\beta(s), 2) \approx 0.611257 \end{aligned}$$

corresponding to whether the magenta points are outside or inside the circumcircle of the red points. It is straightforward to check via computer algebra that these solutions do not satisfy (7) and that the point sets corresponding to these solutions are all distinct.

Finally, we need to show that the purple points lie on the intersections of four lines. To do so, we again compute two determinants corresponding to magenta, green and yellow lines concurrent, and red, green, and yellow lines concurrent, which turn out to be even higher-degree polynomials in  $x$  and  $z$ :

$$\begin{aligned} \det 3 &= \det(m_{-q} \ g_0 \ y_0) \\ &= -36\sqrt{3}(z-1) \left( 3x^7z^4 + 3x^7z^3 + 3x^7z^2 - 6x^6z^4 - 15x^6z^3 - 15x^6z^2 \right. \\ &\quad \left. + 5x^5z^4 + 31x^5z^3 + 27x^5z^2 - 2x^5z - x^5 + 2x^4z^4 - 40x^4z^3 \right. \\ &\quad \left. - 25x^4z^2 + 6x^4z + 3x^4 - 8x^3z^4 + 34x^3z^3 + 13x^3z^2 - 8x^3z - 3x^3 + 8x^2z^4 \right. \\ &\quad \left. - 20x^2z^3 - 3x^2z^2 + 6x^2z + x^2 - 4xz^4 + 8xz^3 - xz^2 - 2xz + z^4 - 2z^3 + z^2 \right) \end{aligned}$$

and

$$\begin{aligned} \det 4 &= \det(r_0 \ g_0 \ y_0) \\ &= -108(z-1)^3 (3x^{12}z^5 + 3x^{12}z^4 + 3x^{12}z^3 - 9x^{11}z^5 + 9x^{11}z^4 \\ &\quad + 9x^{11}z^3 + 9x^{11}z^2 + 6x^{10}z^5 - 108x^{10}z^4 - 123x^{10}z^3 - 63x^{10}z^2 - 3x^{10}z \\ &\quad + 35x^9z^5 + 377x^9z^4 + 422x^9z^3 + 182x^9z^2 + 11x^9z - x^9 - 129x^8z^5 \\ &\quad - 782x^8z^4 - 821x^8z^3 - 306x^8z^2 - 17x^8z + 4x^8 + 246x^7z^5 \\ &\quad + 1112x^7z^4 + 1059x^7z^3 + 339x^7z^2 + 14x^7z - 6x^7 - 318x^6z^5 - 1145x^6z^4 \\ &\quad - 953x^6z^3 - 255x^6z^2 - 5x^6z + 4x^6 + 300x^5z^5 + 866x^5z^4 + 602x^5z^3 + 126x^5z^2 \\ &\quad - x^5z - x^5 - 210x^4z^5 - 476x^4z^4 - 258x^4z^3 - 36x^4z^2 + x^4z + 108x^3z^5 \\ &\quad + 182x^3z^4 + 68x^3z^3 + 4x^3z^2 - 39x^2z^5 - 44x^2z^4 - 8x^2z^3 + 9xz^5 + 5xz^4 - z^5). \end{aligned}$$

Evaluating each of these determinants using the exact solutions found above (and the power of *Mathematica's* symbolic algebra computations) shows that both these determinants evaluate to exactly 0, showing that the four lines  $r_0, g_0, y_0$ , and  $m_{-q}$  are concurrent, at a point we label  $P_0$  (and by symmetry, the other two quadruples of lines are concurrent at  $P_1, P_2$ ).

## 6 Polycyclic realizations of the $(21_4)$ Grünbaum–Rigby configuration

The construction and investigation of  $B(21_4)$  can be generalized in several ways; here we outline some possibilities.

### 6.1 Changing the voltage assignments in $RLG(B)$

We systematically explored all voltage assignments that gave rise to a Levi graph of some combinatorial  $(21_4)$  configuration over the quotient graph  $RLG(B)$  with generic parameters shown in Figure 4b. Two of the authors independently wrote computer programs (TP in *Sage*; LWB in *Mathematica*) that checked all possible values of the parameters

$$\{a, c, d, e, f, g, q, a', c', d', e', f', g', q', t\}$$

over  $\mathbb{Z}_3$ , and eliminated parameter lists that produced Levi graphs with girth less than 6 and isomorphic graphs. We found 17 such Levi graphs. Their parameters are shown in Table 2. Line 1 in this table corresponds to  $RLG(B)$ , while line 3 corresponds to the Grünbaum–Rigby configuration with three-fold (rather than seven-fold) rotational symmetry; that is, line 3 provides parameter values for the reduced Levi graph shown in Figure 4b for which the corresponding Levi graph is isomorphic to the Levi graph of the Grünbaum–Rigby configuration.

However, there is no *strong realization* of the reduced Levi graph with those parameters: that is, every realization of the Grünbaum–Rigby configuration over  $RLG(B)$  has

symmetry classes of points which coincide with each other, which we demonstrate by the following proposition.

**Proposition 6.** *The Grünbaum-Rigby configuration admits only one strong realization as a polycyclic geometric configuration.*

The proof uses a computer but could, in principle, be determined by hand.

*Proof.* As we indicated above, there are only two non-isomorphic polycyclic reduced Levi graphs for the Grünbaum-Rigby configuration. This gives rise to two polycyclic combinatorial realizations, one with seven-fold symmetry and the other one with three-fold symmetry. The configuration with seven-fold symmetry is polycyclically geometrically realizable in essentially only one way (see [1, 16]). A sketch of the argument is that any polycyclic realization of the reduced Levi graph given in Figure 1 is a celestial configuration with symbol  $m\#(s_1, t_1; s_2, t_2; s_3, t_3)$ , which must satisfy the cosine condition and three other conditions, described in [16, Theorem 3.7.1]. However, the only solutions to the cosine condition for  $m = 7$  are cyclic permutations of  $m\#(2, 1; 3, 2; 1, 3)$  and  $m\#(3, 1; 2, 3, 1, 2)$ , which produce congruent geometric configurations.

For three-fold rotational symmetry, *Mathematica*-based symbolic calculations show that the configuration is not geometrically realizable. To see this, use the same pathway and point and line coordinate assignments through the reduced Levi graph described in equation (6), only this time using the parameter assignments

$$\{a, c, d, e, f, g, q, a', c', d', e', f', g', q', t\} = \{1, 2, 0, 1, 1, 2, 2, 1, 2, 0, 1, 1, 2, 2, 0\}$$

given in Table 2 line 3. In this case, similarly to the previous construction, we define

$$\begin{aligned} \det 1 &= \det(R_{d'} C_f B_0) \\ &= (2x^2z + x^2 - 2xz - x + z) (3x^4z^2 - 6x^3z^2 - x^2z^3 + 6x^2z^2 \\ &\quad - x^2 + xz^3 - 3xz^2 + x - z^3 + 2z^2 - z) \end{aligned}$$

and

$$\begin{aligned} \det 5 &= \det(M_0 M_{a'} G_d) \\ &= (12x^{10}z^5 + 3x^{10}z^4 + 12x^{10}z^3 - 60x^9z^5 \\ &\quad - 15x^9z^4 - 60x^9z^3 + 158x^8z^5 + 35x^8z^4 \\ &\quad + 128x^8z^3 - 16x^8z^2 - 4x^8z - 4x^8 - 272x^7z^5 \\ &\quad - 50x^7z^4 - 152x^7z^3 + 64x^7z^2 + 16x^7z + 16x^7 \\ &\quad + 334x^6z^5 + 44x^6z^4 + 96x^6z^3 - 112x^6z^2 - 32x^6z \\ &\quad - 24x^6 - 302x^5z^5 - 20x^5z^4 - 8x^5z^3 + 112x^5z^2 \\ &\quad + 40x^5z + 16x^5 + 203x^4z^5 - 4x^4z^4 - 40x^4z^3 \\ &\quad - 72x^4z^2 - 28x^4z - 4x^4 - 100x^3z^5 + 13x^3z^4 \\ &\quad + 36x^3z^3 + 32x^3z^2 + 8x^3z + 35x^2z^5 - 10x^2z^4 \\ &\quad - 16x^2z^3 - 8x^2z^2 - 8x^2z^5 + 4xz^4 + 4xz^3 + z^5 - z^4). \end{aligned}$$

Solving the system  $\{\mathbf{det1} = 0, \mathbf{det5} = 0\}$  leads to the five real solutions

$$\{x = 0, z = 0\}, \{x = 0, z = 1\}, \{x = 1, z = 0\}, \{x = 1, z = 1\}, \left\{x = \frac{1}{2}, z = \frac{2}{3}\right\},$$

but all of these solutions lead to coinciding points and lines, and thus only a degenerate geometric realization of the configuration.  $\square$

**Theorem 7.** *The configuration B(21<sub>4</sub>) is the only (21<sub>4</sub>) configuration with a nondegenerate  $\mathbb{Z}_3$  geometric polycyclic realization.*

*Proof.* As in the previous proposition, we analyzed all 17 parameter lists given in Table 2, using the same point and line coordinate assignments through the reduced Levi graph described in equation (6) for each set of parameters. In each case, we assigned  $\mathbf{det1} = \det(R_{d'} C_f B_0)$  and  $\mathbf{det5} = \det(M_0 M_{a'} G_d)$  and found all solutions to the system

$$\{\mathbf{det1} = 0, \mathbf{det5} = 0\}. \quad (9)$$

The B configuration #1 and the GR configuration #3 have been analyzed above. Of the remaining configurations, #4, #5, #6, #8, #10, #11, #12, #15, #16 only have degenerate solutions to (9) (that is, all solutions lead to coinciding sets of points and lines).

For the remaining configurations #2, 7, 9, 13, 14, 17, as in the analysis of B, we then evaluated the two determinants

$$\mathbf{det3} = \det(m_{-q} g_0 y_0) \text{ and } \mathbf{det4} = \det(r_0 g_0 y_0) \quad (10)$$

at the nondegenerate solutions to equation (9). These two determinants must both evaluate to exactly 0 in order for the four lines  $m_{i-q}$ ,  $g_i$ ,  $y_i$ ,  $r_i$  to pass through each purple point  $P_i$ .

The determinants in equation (10) for configurations #2, 7, 14, 17 evaluated to numbers that were very far from 0 (on the order of  $10^7$ ). In contrast, the values of the determinants for #9, #13 were numerically both between 0 and 1; however, computing the values of the determinants exactly showed (eventually) that they were not identically equal to 0 and thus, there is no nondegenerate geometric polycyclic realization of either configuration. Pictures of both of these configurations are shown in Figure 10.  $\square$

**Corollary 8.** *There are exactly two geometric polycyclic (21<sub>4</sub>) configurations.*

*Proof.* The configuration B(21<sub>4</sub>) can be polycyclically geometrically realized with  $\mathbb{Z}_3$  symmetry, and the configuration GR(21<sub>4</sub>) can be polycyclically geometrically realized with  $\mathbb{Z}_7$  symmetry. Since the only two possible reduced Levi graphs have each been analyzed and there are no other parameter values that lead to nondegenerate realizations, it follows that these are the only two geometric polycyclic configurations.  $\square$

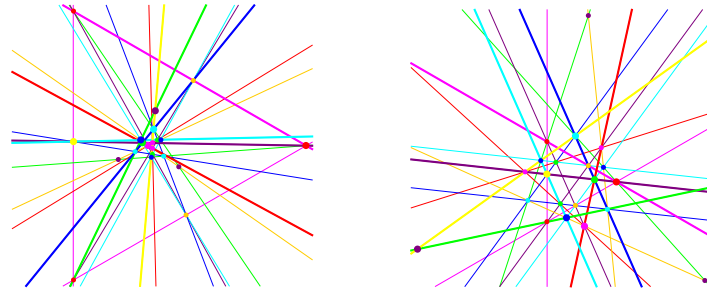


Figure 10: Configurations #9 (left) and #13 (right) have at least one nondegenerate realization that satisfies Equation (9), which means that points  $R_{d'}, C_f, B_0$  are collinear (on the thick green line) and points  $M_0, M_{a'}, G_d$  are collinear (on the thick red line). However, because the determinants in equation (10) are not identically equal to 0, the purple points do not lie on the common intersection of four lines. In these drawings, the purple points  $P_i$  are defined as the intersection of lines  $y_i$  and  $g_i$ , and the 0th element of each class is shown large (for points) or thick (for lines).

item	$\{a, c, d, e, f, g, q, a', c', d', e', f', g', q', t\}$	Aut	name	self-dual?	NDSols?
1	$\{1, 2, 0, 1, 1, 1, 2, 1, 2, 0, 1, 1, 1, 2, 0\}$	12	B	y	Y
2	$\{1, 2, 0, 1, 1, 1, 2, 1, 2, 0, 1, 1, 2, 2, 0\}$	6		y	y
3	$\{1, 2, 0, 1, 1, 2, 2, 1, 2, 0, 1, 1, 2, 2, 0\}$	672	GR	y	n
4	$\{1, 2, 0, 1, 1, 1, 2, 1, 2, 0, 2, 2, 1, 2, 0\}$	12		y	n
5	$\{1, 2, 0, 1, 1, 1, 2, 1, 2, 0, 2, 2, 2, 2, 0\}$	12		y	n
6	$\{1, 2, 0, 1, 1, 1, 0, 1, 2, 2, 1, 1, 1, 2, 0\}$	6		y	n
7	$\{1, 2, 0, 1, 1, 1, 0, 1, 2, 2, 1, 1, 2, 2, 0\}$	6		y	y
8	$\{1, 2, 0, 1, 1, 1, 0, 1, 2, 2, 2, 2, 1, 2, 0\}$	12		y	n
9	$\{1, 2, 0, 1, 1, 1, 0, 1, 2, 2, 2, 2, 2, 2, 0\}$	3		n	y
10	$\{1, 2, 0, 1, 1, 2, 0, 1, 2, 2, 2, 2, 2, 2, 0\}$	6		y	n
11	$\{1, 2, 0, 2, 2, 1, 0, 1, 2, 2, 2, 2, 2, 2, 0\}$	6		y	n
12	$\{1, 2, 0, 2, 2, 2, 0, 1, 2, 2, 2, 2, 1, 2, 0\}$	6		y	n
13	$\{1, 2, 0, 2, 2, 2, 0, 1, 2, 2, 2, 2, 2, 2, 0\}$	12		y	y
14	$\{1, 2, 2, 1, 1, 1, 0, 1, 2, 2, 2, 2, 2, 0, 0\}$	6		y	y
15	$\{1, 2, 2, 1, 1, 2, 0, 1, 2, 2, 2, 2, 2, 0, 0\}$	24		y	n
16	$\{1, 2, 2, 2, 2, 1, 0, 1, 2, 2, 2, 2, 2, 0, 0\}$	12		y	n
17	$\{1, 2, 1, 1, 1, 1, 0, 2, 1, 2, 2, 2, 2, 0, 0\}$	6		y	y

Table 2: Parameters of Levi graphs of all 17 combinatorial configurations derived from  $\text{RLG}(\text{B})$ , with parameters corresponding to those in 4b. Lines 1 and 3 (highlighted in gray) correspond to B and GR respectively. The column  $|\text{Aut}|$  gives the number of automorphisms of the Levi graph. The column “self-dual?” indicates whether the configuration is combinatorially self-dual, and the column “NDSols” indicates whether there are any non-degenerate solutions to the system  $\{\det 1 = 0, \det 5 = 0\}$  (see text); the annotation ‘y’ says that there are non-degenerate solutions that do not lead to a full geometric realization, while ‘Y’ says that there are non-degenerate solutions that **do** lead to a full geometric realization.

It is interesting that among the 17 non-isomorphic Levi graphs, 16 give rise to self-dual combinatorial configurations. Only one Levi graph, defined by parameters in Table 2 line #9, gives rise to a pair of dual configurations, bringing the total of non-isomorphic configurations to 18. A Levi graph admits a self-dual configuration if and only if it has an automorphism that interchanges the sets of bipartition. One would expect that in such a situation, the dual pair of configurations would give rise to two sets of parameters. However, this is not the case here. Namely, the dual pair of configurations have isomorphic underlying Levi graphs (with vertex colors reversed). On the other hand, there is no color-preserving isomorphism that would map one (vertex-colored) Levi graph onto the other one. The opposite is true in all other 16 cases.

## 7 Conclusions and open questions

Since two non-isomorphic geometric  $(21_4)$  configurations exist, and these are the only (strongly) realizable polycyclic geometric  $(21_4)$  configurations, the natural question is: *Are there more of them?* An over-ambitious project involves a solution to the following formal problem.

**Problem 9.** Determine all geometric  $(21_4)$  configurations.

The complete solution to this problem seems to be out of reach with our current knowledge about configurations. The brute-force approach does not seem feasible. Namely, no one knows how many combinatorial  $(21_4)$  configurations exist. It is not known how many connected bipartite graphs of girth at least 6 on 42 vertices exist. The number must be large, since it is known that there exist almost two billion distinct quartic graphs of girth at least 6 on 38 vertices. Since the numbers grow exponentially, bridging the gap between 38 and 42 seems to be intractable. One has to abandon the idea of determining first the collection of all combinatorial  $(21_4)$  configurations and in the second step filtering out configurations that admit geometric realization.

It seems wiser to set up a more modest goals that we state as a problem.

**Problem 10.** Determine all geometric  $(21_4)$  configurations with non-trivial geometric symmetry.

**Question 11.** Does there exist a geometric  $(21_4)$  configuration that has no polycyclic realization?

### 7.1 Changing the voltage group

Another way to generalize  $B(21_4)$  is to change the voltage group of  $RLG(B)$  from  $\mathbb{Z}_3$  to  $\mathbb{Z}_m$ , for some  $m > 3$ . This is equivalent to saying that one expects an infinite series of configurations with rotational symmetry of order  $m$ , all with analogous structure to that of  $B(21_4)$ .

We made a number of experiments for constructing such examples, using both our synthetic method in Section 3 and the procedure implemented in *Mathematica* described

in Section 5. It is clear that there likely are a number of infinite families of similar configurations. However, to find a proof we have to understand better the structure of these configurations. This is a subject of future research. Based on preliminary experiments, we conjecture

**Conjecture 12.** The following parameter values lead to geometric  $(7m_4)$  configurations, which can be realized polycyclically over  $\mathbb{Z}_m$ :

$$F_1(m; a, b) = \{a, c, d, e, f, g, q, a', c', d', e', f', g', q', t\} = \{a, -a, a, b, b, -a, -2a, a, -a, a, b, b, -a, -2a, 0\} \quad (11)$$

for  $a \geq b, 1 \leq a, b \leq m/2$ , and

$$F_2(m; a, b) = \{a, c, d, e, f, g, q, a', c', d', e', f', g', q', t\} = \{a, b, b, b, b, b, b, a, b, b, b, b, b, b, 0\} \quad (12)$$

for  $a \geq b, a \neq m/2$ , although there may be other constraints on  $a$  and  $b$  that have not yet been identified.

We conjecture that there are other valid as-yet-unidentified parameter families as well.

Note that the configuration  $F_1(3; 1, 1)$ , with the parameters given in (11), is isomorphic to  $B(21_4)$ .

We have numerically verified the existence of configurations in both parameter families for many values of  $m$ ; they have been verified exactly for  $m = 4, 6$  using the process given in section 5 (with the corresponding parameter values, naturally). Figures 11 and 12 show several examples of such configurations, in both conjectured parameter families. There are many other such examples.

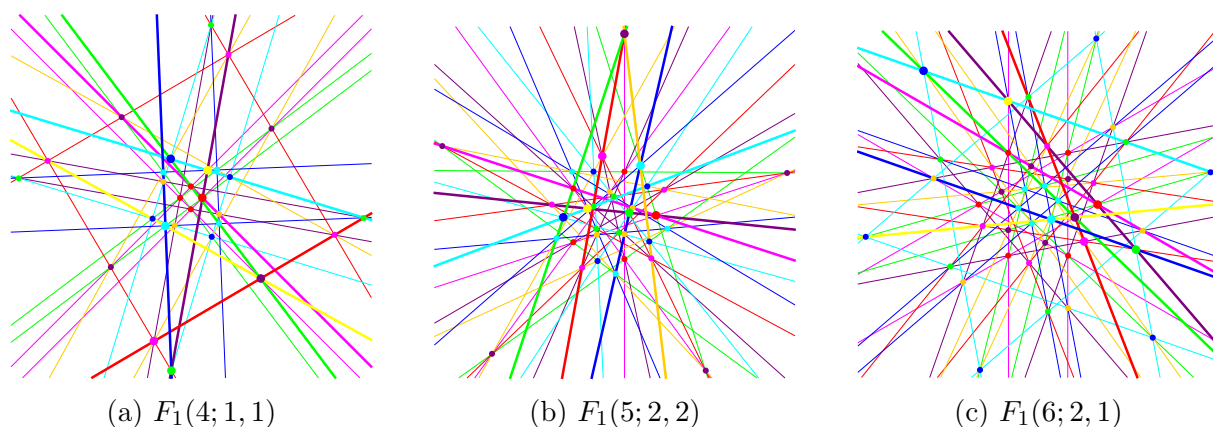


Figure 11: Examples of configurations in family  $F_1(m; a, b)$ .



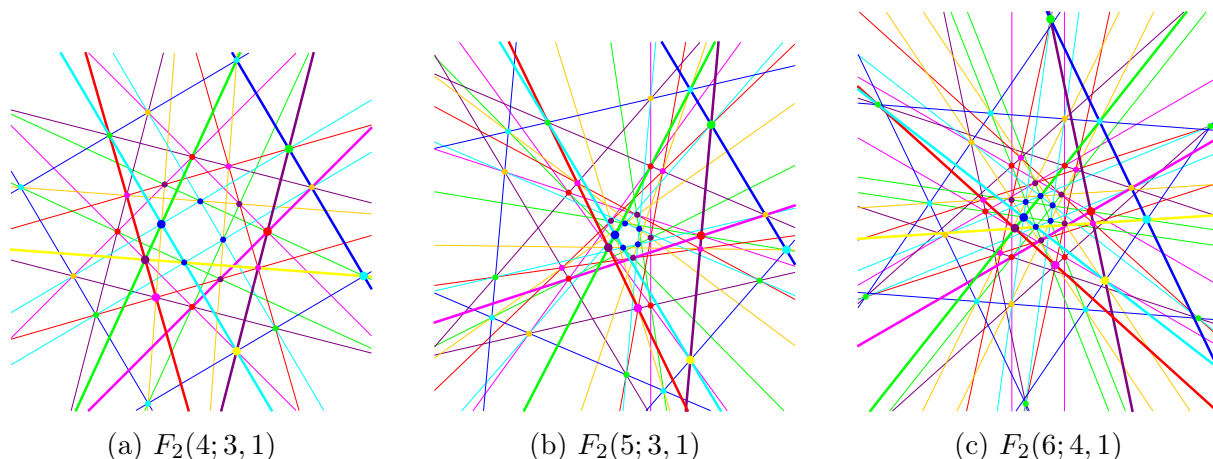


Figure 12: Examples of configurations in family  $F_2(m; a, b)$ .

## Acknowledgements

Gábor Gévay is supported by the Hungarian National Research, Development and Innovation Office, OTKA grant No. SNN 132625. Tomaž Pisanski is supported in part by the Slovenian Research Agency (research program P1-0294 and research projects J1-1690, N1-0140, J1-2481).

## References

- [1] A. Berardinelli and L. W. Berman. Systematic celestial 4-configurations. *Ars Math. Contemp.*, 7(2):361–377, 2014.
- [2] L. W. Berman. Geometric constructions for 3-configurations with non-trivial geometric symmetry. *Electron. J. Combin.*, 20(3):#P9, 29, 2013.
- [3] L. W. Berman, P. DeOrsey, J. R. Faudree, T. Pisanski, and A. Žitnik. Chiral astral realizations of cyclic 3-configurations. *Discrete Comput. Geom.*, 64(2):542–565, 2020.
- [4] L. W. Berman, J. R. Faudree, and T. Pisanski. Polycyclic movable 4-configurations are plentiful. *Discrete Comput. Geom.*, 55(3):688–714, 2016.
- [5] L. W. Berman, E. Jacksch, and L. Ver Hoef. An infinite class of movable 5-configurations. *Ars Math. Contemp.*, 10(2):411–425, 2016.
- [6] M. Boben and T. Pisanski. Polycyclic configurations. *European J. Combin.*, 24(4):431–457, 2003.
- [7] J. Bokowski and V. Pilaud. On topological and geometric  $(19_4)$  configurations. *European J. Combin.*, 50:4–17, 2015.
- [8] J. Bokowski and V. Pilaud. Quasi-configurations: building blocks for point-line configurations. *Ars Math. Contemp.*, 10(1):99–112, 2016.

- [9] J. Bokowski and L. Schewe. There are no realizable  $15_4$ - and  $16_4$ -configurations. *Rev. Roumaine Math. Pures Appl.*, 50(5-6):483–493, 2005.
- [10] J. Bokowski and L. Schewe. On the finite set of missing geometric configurations  $(n_4)$ . *Comput. Geom.*, 46(5):532–540, 2013.
- [11] H. S. M. Coxeter and S. L. Greitzer. *Geometry Revisited*. The Mathematical Association of America, Washington, DC, 1967.
- [12] H. S. M. Coxeter. *Introduction to Geometry*. Wiley, New York, 2nd edition, 1969.
- [13] H. L. Dorwart and B. Grünbaum. Are these figures oxymora? *Math. Mag.*, 65(3):158–169, 1992.
- [14] G. Gévay and P. Pokora. Klein’s arrangements of lines and conics. *Beiträge Algebra Geom.*, 2023.
- [15] B. Grünbaum. Musings on an example of Danzer’s. *European J. Combin.*, 29(8):1910–1918, 2008.
- [16] B. Grünbaum. *Configurations of Points and Lines*, volume 103 of *Graduate Studies in Mathematics*. American Mathematical Society, Providence, RI, 2009.
- [17] B. Grünbaum and J. F. Rigby. The real configuration  $(21_4)$ . *J. London Math. Soc.*, 41:336–346, 1990.
- [18] B. Grünbaum and G. C. Shephard. Is selfduality involutory? *Amer. Math. Monthly*, 95:729–733, 1988.
- [19] F. Klein. Ueber die Transformation siebenter Ordnung der elliptischen Funktionen. *Math. Ann.*, 14(3):428–471, 1878.
- [20] T. Pisanski and B. Servatius. *Configurations from a Graphical Viewpoint*. Birkhäuser Advanced Texts. Birkhäuser, New York, 2013.